Intrinsically anomalous roughness of randomly crumpled thin sheets

Alexander S. Balankin, Orlando Susarrey Huerta, Rolando Cortes Montes de Oca, Didier Samayoa Ochoa, José Martínez Trinidad, and Maribel A. Mendoza

Grupo "Mecánica Fractal," Instituto Politécnico Nacional, México D.F., 07738 Mexico

(Received 3 April 2006; revised manuscript received 3 October 2006; published 7 December 2006)

We study the effect of folding ridges on the scaling properties of randomly crumpled sheets of different kinds of paper in the folded and unfolded states. We found that the mean ridge length scales with the sheet size with the scaling exponent μ determined by the competition between bending and stretching deformations in the folded sheet. This scaling determines the mass fractal dimension of randomly folded balls $D_M=2/\mu$. We also found that surfaces of crumpled balls, as well as unfolded sheets, both display self-affine invariance with $\zeta=\nu_{\mathrm{ph}}$, if $\mu\leqslant\nu_{\mathrm{ph}}$, where $\nu_{\mathrm{ph}}=3/4$ is the size exponent for crumpled phantom membrane, or both exhibit an intrinsically anomalous roughness characterized by the universal local roughness exponent $\zeta=0.72\pm0.04$ and the material dependent global roughness exponent $\alpha=\mu$, when $\mu>\nu_{\mathrm{ph}}$. The physical implications of these findings are discussed.

DOI: 10.1103/PhysRevE.74.061602 PACS number(s): 68.03.Cd, 68.35.Ct, 05.45.Df, 89.75.Da

I. INTRODUCTION AND BACKGROUND

In the past decade, there has been a great deal of interest in crumpling processes, ranging from the folding of blood cell's membranes to the Earth's crust buckling. In particular, the statistical geometry of randomly crumpled membranes and sheets has drawn much attention [1–3]. It was found that all thin sheets of just about any material crumple in the same way, such that the stress energy is concentrated in the network of narrow ridges (folding creases) [4,5]. This leads to anomalously low compressibility of folded sheets [6] and to a very slow stress-strain relaxation in crumpled materials [6,7]. Specifically, the diameter of a randomly crumpled paper ball depends on the confinement force as $R\propto F^{-\delta}$, where $\delta\approx0.25$ [8].

Early, it was found that randomly folded sheets exhibit scale invariance, such that the ball mass ($M=\rho_A L^2$, where ρ_A is the surface mass density and L is the sheet size) scales with its averaged diameter R as

$$M\propto R^{D_M}, \tag{1}$$

where D_M is the mass fractal dimension [9]. On the other hand, it was noted that the external surfaces of randomly crumpled sheets also reveal a multiscale roughness within a wide range of length scales [10]. Besides, the roughness of unfolded crumpled sheets is assumed to display a self-affine scaling, characterized by the universal local roughness exponent ζ, also called the Hurst exponent [2,11]. However, the physical nature of crumpling geometry remains poorly understood [12].

Indeed, there is no clarity even about the scaling properties of crumpled elastoplastic sheets in the folded and unfolded states. In particular, many authors, e.g. [7], have explicitly assumed that the folded state of randomly crumpled thin sheets is characterized by the universal fractal dimension $D_M^{\mathrm{Flory}}=2.5$ determined by self-avoidance of a two-dimensional sheet in three-dimensional space [13]; nevertheless, the experimental values of D_M range from 2.1 to 2.8 for a crumpled ball made from sheets of different materials [14]. On the other hand, the dimensional analysis of the results of computer simulations has suggested that the fractal dimension of balls of randomly crumpled thin sheets [$(h/L)^2<10^{-5}$, where h is the sheet thickness] is determined by the scaling relation [8]

$$R\propto L^{\nu}F^{-\delta}, \tag{2}$$

where the scaling exponents δ and $\nu=2/D_M$ are expected to take the universal values for phantom ($\delta=3/8$, $\nu_{\mathrm{ph}}=3/4$; $D_M=8/3$) and self-avoiding ($\delta=1/4$, $\nu_{\mathrm{sa}}=0.8$; $D_M^{\mathrm{Flory}}=2.5$) membranes characterized by the dimensionless Föppl–von Kármán number $\gamma=EL^2/\kappa\propto(L/h)^2\rightarrow\infty$ [8] (here E is the Young modulus, $\kappa=cEh^2$ is the bending rigidity of sheets, and $c\approx1$ is a function of Poisson ratio). In the case of finite γ, the crumpled configurations of elastoplastic sheets are essentially nonequilibrium, and so one can expect deviation from the Flory approximation [15,16]. However, the computer simulations [8] do not detect the effect of bending rigidity on the values of scaling exponents. Furthermore, there is also a controversy about the scaling properties of unfolded sheet roughness [17]. Namely, quite recently, it was suggested that $\zeta=0.71\pm0.01$ [2], in contrast with the value of $\zeta=0.88\pm0.06$ reported previously in [11]. Besides, as far as we know, the effect of the ridge network on the scaling properties of crumpled sheets has never been studied.

Accordingly, the aim of this work was to ascertain the nature of crumpling patterns and to establish the interrelationships between different scaling exponents characterizing the geometrical properties of randomly crumpled sheets in the folded and unfolded states.

II. EXPERIMENTS

Experiments with paper offer a convenient, economical means of studying crumpling phenomena in the laboratory [2,9–11,18–20]. Accordingly, to get an insight into the geometry of crumpling, in this work we performed a study of scaling properties of hand crumpled paper sheets of different bending rigidity (see Table I) in both the folded [see Fig. 1(a)] and unfolded [see Fig. 1(b)] states. Moreover, we have

TABLE I. Thickness (h), surface density (ρ_A), Young moduli (E_L, E_T), and yield stresses (σ_{YL}, σ_{YT}) of papers (subindices denote the direction of measurement: L along and T across the machine direction of paper), and the scaling exponents characterizing crumpled sheets. Notice that all papers have the same mass density: $\rho=\rho_A/h=900\pm50$ kg/m^3.

Commercial name of paper	Carbon	Copia	Biblia	Albanene-1	Albanene-2
h (mm)	0.024±0.004	0.030±0.003	0.039±0.002	0.068±0.005	0.087±0.005
ρ_A (g/m^2)	22±0.8	27±1	35.6±0.5	63±1	80±2
E_L (MPa)	3155±175	3500±150	3931±144	7102±200	7250±200
E_T (MPa)	1860±232	1950±200	1355±65	4036±87	4100±100
σ_{YL} (MPa)	34.6±2	35.5±2	37.5±0.7	56.8±3	60±3
σ_{YT} (MPa)	11.9±0.5	15.4±1	23.4±1	41±1	45±3
D_M	2.13±0.05	2.25±0.05	2.30±0.05	2.54±0.06	2.72±0.06
ζ_B	0.72±0.04	0.72±0.04	0.71±0.03	0.72±0.02	0.71±0.04
α_S	0.94±0.03	0.88±0.04	0.86±0.03	0.79±0.02	0.73±0.02
ζ_L	0.70±0.04	0.71±0.03	0.71±0.04	0.71±0.05	0.71±0.05
α_L	0.93±0.02	0.89±0.02	0.87±0.03	0.79±0.01	0.74±0.02
μ	0.95±0.1	0.90±0.1	0.85±0.05	0.78±0.06	0.72±0.05

also studied the statistical geometry of the networks of folding ridges clearly observed when the unfolded sheet is flattened [see Fig. 1(c)].

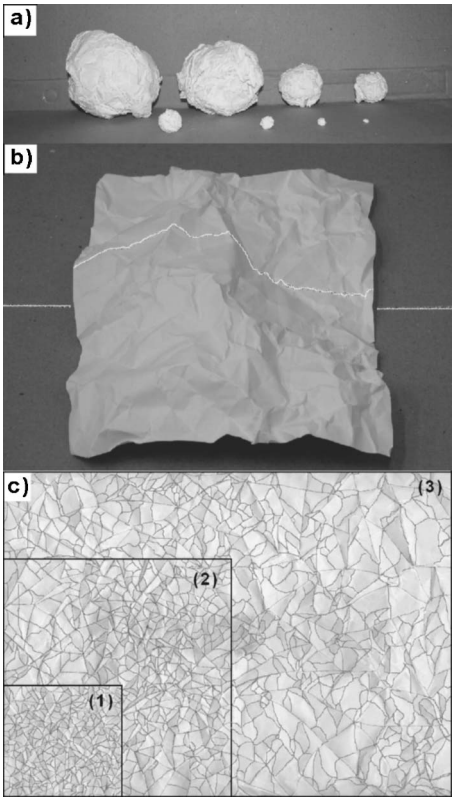

FIG. 1. The images of (a) crumpled balls from the Biblia paper sheets of different sizes and (b) the unfolded state of a crumpled sheet of Albanene-1 paper of size $L=35$ cm (white curve—the intersection of light sheet with crumpled paper sheet). (c) Ridge networks formed in flattened crumpling sheets of size $L=8$ (1), 16 (2), and 35 (3) cm of Albanene-1 paper.

A. Experimental details

In this work we studied the fractal geometry of randomly crumpled sheets of five different kinds of paper characterized by different thickness h and bending rigidity $\kappa=cEh^2$ (see Table I). For this purpose the square sheets of paper with edge size L were crumpled in hands into approximately spherical balls of diameter $R(L)$. The sheet size was varied from $L_0=2$ to 100 cm with the relation $L=\lambda L_0$ for scaling factor $\lambda=1$, 2, 4, 8, 16, 20, 32, and 50 [see Fig. 1(a)]. Notice that for sheets used in this work the ratio $(h/L)^2$ varies in the range from 6×10^{-8} to 2×10^{-5}. At least $N=30$ sheets of each size of each kind of paper were folded.

The mean diameter $\overline{R_j(L)}=(1/n)\Sigma_i^n R_i$ of each ball and its standard deviation $\sigma_s\propto(1/\sqrt{n})[\Sigma_i^n(R_i-\overline{R})^2]^{1/2}$ were determined from measurements of R_i along $n=15$ directions taken at random. Further, we calculated the ensemble averaged diameters, $R(L)=\langle\overline{R_j(L)}\rangle$, where the brackets denote average over $N=30$ balls of the same size L, and the corresponding standard deviations $\sigma_B=(1/\sqrt{N})[\Sigma_j^N(\overline{R_j}-R)^2]^{1/2}$. We found that for almost all balls, the distribution of R_i can be well fitted [21] by the inverse Gaussian distribution, while the mean diameters $\overline{R_j(L)}$ follow a normal distribution.

At the initial stage of this study we expect that the diameter of the crumpled ball depends on the sheet size as well as on the squeezing force according to the scaling relation (2) and so, to obtain the ball fractal dimension from the scaling relation (1), we need to reduce the variations in the squeezing force applied to the sheets of different sizes. In practice, however, we noted that the inherent statistical variations of squeezing force in the hand crumpling experiments (±25%) have only a small effect on the ball diameter because of the very slight dependence $R\propto F^{-0.25}$ [8]. Furthermore, we noted that, once the folding force is withdrawn, the ball diameter increases with time during approximately 6–9 days, due to the strain relaxation. In all cases we found that the ball diameter increases as

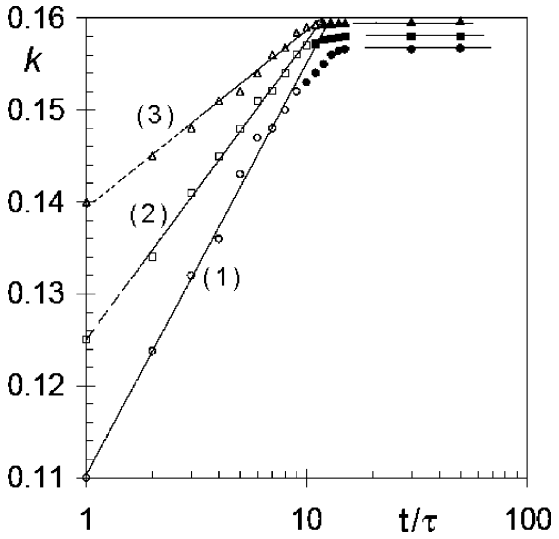

FIG. 2. Graphs of $k(t)$ versus t/τ for balls folded from Albanene-1 paper of size $L=70$ cm with different initial confinements $k_0=0.11\pm0.001$ (1), 0.125 ± 0.002 (2), and $0.1.4\pm0.003$ (3). In all cases the final confinement is $k(t\gg\tau)=0.158\pm0.02$. Points—experimental data averaged over 10 experiments; lines—data fitting with Eq. (3).

$$R(t) = R(0) + \kappa \ln(t/\tau), \tag{3}$$

where the strain relaxation rate (κ) and the characteristic time (τ) are dependent on the initial confinement ratio $k_0 = R(0)/L \propto F^{-\delta}/L^{1-\nu}$, bending rigidity $\kappa = h^2E$, and air humidity. The relative increase in the ball diameter can achieve 30% (see also [7]). Detailed study of strain relaxation in the randomly crumpled sheets will be published elsewhere. Here we only pointed out the finding that after strain relaxation during 10 days the mean diameter of crumpled ball $R(t\gg\tau)$ is almost independent of the initial confinement ratio [22] and air humidity varies in the range from 25% to 35% [23], at least for the balls with initial confinement ratio in the range $0.1<k_0<0.3$ (see Fig. 2). Hence, to reduce the uncertainties caused by variations in the squeezing force and strain relaxation, all measurements reported below were performed ten days after the balls were folded, when no changes in the ball dimensions were observed.

The mass fractal dimensions of the crumpled ball series were determined from the scaling behavior (1), where D_M is found to be different for crumpled balls of different kinds of paper [see Fig. 3(a) and Table I]. To characterize the roughness of the ball surface, we note that the global roughness of balls scales with the ball diameter as

$$\sigma_B \propto \sigma_S \propto R^{\alpha_S}, \tag{4}$$

where α_S is the global roughness exponent of spherical balls [see Fig. 3(b)]. Besides, we also studied the local roughness of ball surfaces characterized by the local roughness exponent ζ_S defined by the scaling behavior

$$\sigma_R(\Delta_\theta) = \langle\langle\langle R_i - \langle R_i\rangle_\Delta\rangle_\Delta^2\rangle_{\pi R}^{1/2}\rangle_\varphi \propto \Delta_\theta^{\zeta_s}, \tag{5}$$

where $\langle\cdots\rangle_\Delta$ and $\langle\cdots\rangle_\varphi$ denote the averages within the arc of length Δ_θ and over the angle φ in spherical coordinates [24].

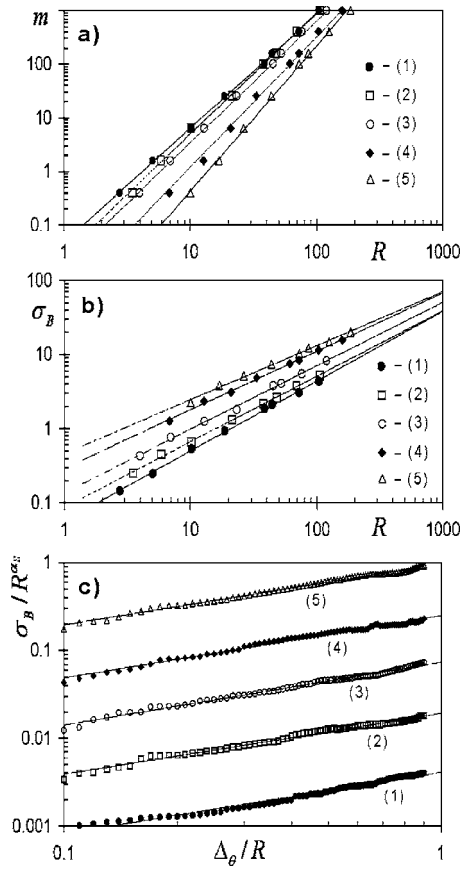

FIG. 3. Log-log plots of (a) $m=M/\rho_A=L^2$ (cm^2), (b) σ_B (mm) versus R (mm), and (c) σ_R/R^{α_s} versus Δ_θ/R (arbitrary units). The numbering corresponds to different papers: Carbon (1), Copia (2), Biblia (3), Albanene-1 (4), and Albanene-2 (4). Notice that the graphs in panel (c) are shifted for clarity.

Further, to study the roughness of unfolded sheets, each ball unfolded up to its height $z(x,y)$ becomes a univalent function of x and y [see Fig. 1(b)]. The unfolded sheet has a rough surface composed by small tiles bounded by folding edges. The global roughness of unfolded sheets can be characterized through the scaling behavior of the standard deviations of the maximum sheet height

$$\sigma_Z(L) = \langle[\Delta z_j - \langle\Delta z_j\rangle_N]^2\rangle_N^{1/2} \propto L^{\alpha_L}, \tag{6}$$

where $\Delta z_j = \max_{x,y\in L} z_j(x,y) - \min_{x,y\in L} z_j(x,y)$ [25]. We found that the statistical distribution of maximum sheet heights conforms to a log-normal distribution [21]. We note that the statistical error associated with the unfolding process practically does not affect the scaling relation (6). Further, to determine the local roughness exponent ζ_L of unfolded crumpled sheets, we obtained 15 profiles $z_i(x)$ of each sheet, with the help of a laser which produces an approximately horizontal sheet of light and a photocamera Coolpix-5700 with a resolution of 2560×1920 pixels (see also [2]). After an appropriate calibration (see [2]) the bright curves of light reflection [see Fig. 1(b)] were digitized with the help of Scion Image software [26]. Accordingly, we measured the local width of each profile,

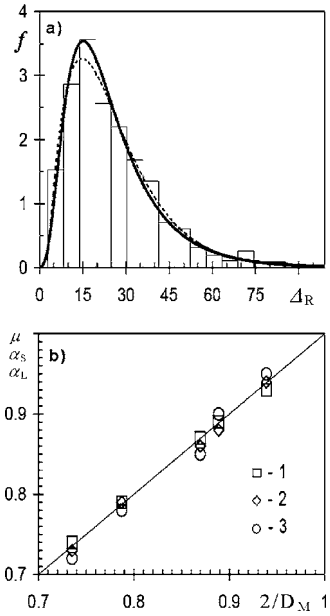

FIG. 4. (a) Statistical distributions of ridge length in an unfolded sheet of Albalene-1 paper size 70×70 cm. Bins—experimental data; solid line—data fitting with log-normal distribution; dashed line—data fitting with gamma distribution (p value =04486). (b) Experimental values of exponents μ (1), α_S (2), and α_L (3) plotted versus $\nu=2/D_M$.

$$\sigma_L = \langle\langle [z(x) - \langle z\rangle_\Delta]^2\rangle_\Delta\rangle_L^{1/2} \propto \Delta^{\zeta_L}, \tag{7}$$

where $\langle\cdots\rangle_\Delta$ denotes an average over x in windows of size Δ.

The crumpling is an irreversible process, and so, a crumpled elastic-plastic sheet can never be perfectly smoothed again. Indeed, in the smoothed sheet we can observe the network of creases of different lengths [see Fig. 1(c)]. To characterize the statistical geometry of the folding network we studied the crease-length distribution in sheets of different sizes. We found that the crease-length distribution is best fitted [21] by the log-normal distribution [see Fig. 4(a) [27]]. This is consistent with experimental observations [2], computer simulations [8], and theoretical model [5] based on the hierarchical splitting of a ridge during sheet folding.

B. Scaling analysis

First of all, we found that the density of crumpled balls scales with the ball diameter as

$$\rho_B = \rho_0 (R/h)^{D_M-3} \tag{8}$$

for $R_B \gg h$, where ρ_0 is a decreasing function of the bending rigidity of paper (see Table I). Besides, we noted that for the hand-folded sheets with low bending rigidity the experimental values of D_M are considerably less than the universal value $D_M^{\text{Flory}}=2.5$, whereas for the more rigid sheets we found $D_M > D_M^{\text{Flory}}=2.5$ (see Table I).

The global roughness of crumpled balls (4) is also characterized by the material dependent global roughness exponent. Moreover, we found that experimental values of α_S and D_M (see Table I) are consistent with the empirical relationship [see Fig. 4(b)]:

$$\alpha_S = \nu = 2/D_M, \tag{9}$$

indicating that the surface roughness of the crumpled paper balls scales as $\sigma_B \propto \sigma_S \propto R^{\alpha_S} \propto L$.

It should be pointed out that, generally, the surface roughness is characterized by different scaling exponents in the local and global scales $\alpha \geq \zeta$ [28,29]. Self-affine surfaces are characterized by the unique roughness exponent, also called the Hurst exponent $H=\alpha=\zeta$, which is related to the box-counting fractal dimension of the surface as $D_B=3-H$ [30], whereas the true area of the self-affine surface is characterized by the divider fractal dimension $D_D=2/H$, if $H>2/3$, or $D_D=3$, if $H\leq 2/3$ [30]. Hence, in the case of self-affine invariance of the ball surface ($\alpha_S=\zeta_S$), relation (9) implies that the divider fractal dimension of the crumpled surface is equal to the mass fractal dimension of the ball. In contrast to this, the roughness characterized by different scaling exponents in the local and global scales ($\alpha > \zeta$) is called anomalous. There are different types of anomalous roughness which were classified within the concept of a generic dynamic scaling ansatz [28]. Therefore, to determine the nature of ball roughness, we also studied the local roughness of ball surfaces (5). We found that the local roughness of all balls is characterized by the same universal local roughness exponent $\zeta_S=0.72\pm0.04$. Notice that the inequality

$$\zeta_S = 0.72 \pm 0.04 < \alpha_S = 2/D_M < 1 \tag{10}$$

indicates the intrinsically anomalous nature (see [28,29]) of the crumpled ball surface, except in the case of Albanene-2 paper, for which numerically $\alpha_S \approx \zeta_S$. This leads to the following scaling relation [see Fig. 3(c)]:

$$\sigma_R/R^{\alpha_S} \propto \sigma_R/L \propto (\Delta_\theta/R)^{\zeta_S}. \tag{11}$$

On the other hand, we found that the local width of unfolded sheets demonstrates two distinct scaling regions [see Fig. 5(a)]. For intervals smaller than the characteristic ridge length Δ_C we found $\zeta_L \cong 0.95\pm0.15$, indicating the linear geometry of individual ridges (see also Ref. [2]), whereas in larger intervals ($\Delta > \Delta_C$) the local roughness is characterized by the universal local roughness exponent

$$\zeta_L = 0.72 \pm 0.04 = \zeta_S \tag{12}$$

for all kinds of paper (see Table I). Besides, we noted that Δ_C increases as sheet size L increases and so the local roughness is also a function of L, such that $\Delta > \Delta_C$ or the local roughness of unfolded sheets scales as [see Fig. 5(b)]

$$\sigma_L/L^{\alpha_L} \propto \sigma_L/R \propto (\Delta/L)^{\zeta_L}, \tag{13}$$

as is expected in the case of intrinsically anomalous roughness (see [28,29]), characterized by the material dependent global roughness exponent

$$\alpha_L = \alpha_S = \nu = 2/D_M \tag{14}$$

(see Table I). This finding is consistent with the sheet size dependence of the global roughness of unfolded sheets, which is found to scale as $\sigma_Z \propto L^{2/D_M} \propto R$ [see Fig. 5(c)].

To get a better insight into the anomalous nature of crumpled sheet roughness, we analyzed the effect of sheet size on the length of folded creases [see Fig. 1(c)]. We found

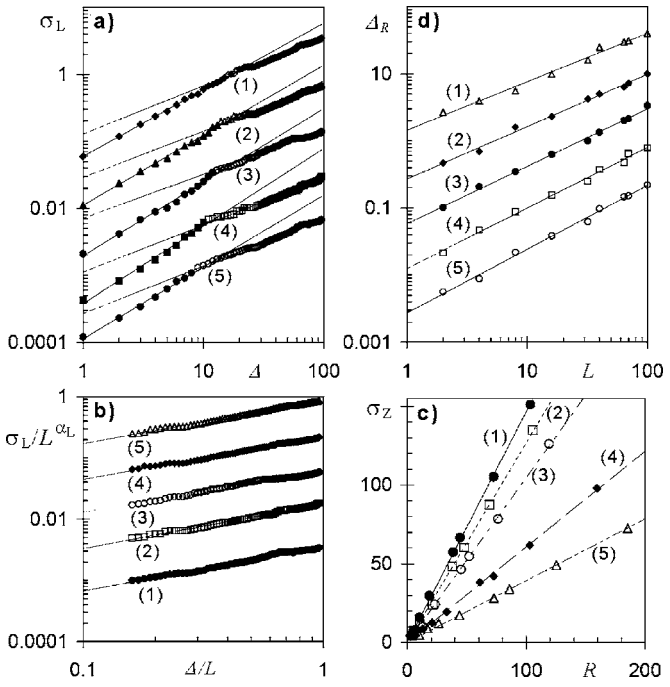

FIG. 5. (a) Plots of σ_Z (mm) versus R_B (mm) and log-log plots of (b) the local width σ_L (mm) of 1D profiles of unfolded sheets of size 50×50 cm versus window size Δ (mm), (c) σ_L/L^{α_L} versus Δ/L (arbitrary units), and (d) the mean ridge length Δ_R (mm) versus sheet size L (mm). The numbering corresponds to different papers: Carbon (1), Copia (2), Biblia (3), Albanene-1 (4), and Albanene-2 (4); notice that the graphs in panels (b)–(d) are shifted for clarity.

that the ensemble averaged length of ridges increases with L [see Fig. 5(d)] as

$$\Delta_R \propto L^{\mu}, \tag{15}$$

where the experimental values of μ (see Table I [31]) are found to be consistent with the empirical relation (see Fig. 5)

$$\mu = \nu = \alpha = 2/D_M, \tag{16}$$

which is also consistent with the scaling behavior of the lower cutoff $\Delta_C \cong \Delta_R$ of sheet roughness (the symbol $\cong$ denotes the equality in the statistical sense).

III. DISCUSSION

Crumpling of thin elastoplastic sheets leads to the formation of complex folding patterns over several length scales. This leads to an intriguing coupling between the mechanics and geometry of crumpling phenomena. Moreover, the fractal structure of crumpled balls determines their elastic properties [32]. Hence, to understand the nature of crumpling processes, it is necessary to understand the scaling geometry of crumpling and its relation to the geometry of the folding network. In this way, this study provides the experimental evidence that the scaling geometry of crumpled sheets in the folded and unfolded states is governed by the scaling properties of folding creases.

Specifically, we found that the mass fractal dimension of randomly folded sheets is determined by power law dependence of folding crease length on the sheet size (15), such that $D_M=2/\mu$. So, taking into account that $2\leq D_M\leq 3$, the admissible range of μ is

$$2/3 \leq \mu = \nu \leq 1. \tag{17}$$

Experimental data from Table I suggest that the value of μ is determined by the competition between the bending and stretching deformations in the folded sheet, such as for papers with larger thickness and bending rigidity $2/3<\mu<\nu_{\rm ph}=0.75$, whereas for more flexible and thin papers, $\mu>\nu_{\rm sa}=4/5=0.8$. We note that for self-avoiding sheets with finite bending rigidity numerical simulations predict $\nu_{\rm sa}^R=0.87>\nu_{\rm sa}$; nevertheless, the dependence of ν on sheet rigidity was not detected [8]. These simulations also suggest that the crumpled ball confinement ratio depends on the sheet rigidity as [8]

$$k_0 \propto \gamma^{\beta}\left(\frac{\kappa}{FL}\right)^{\delta}, \tag{18}$$

and so the size exponent is equal to

$$\nu = 2\beta + 1 - \delta, \tag{19}$$

where exponent β is determined by the self-avoiding interactions [8].

When the thickness of the sheet is diminished without limit, the deformations associated with sheet crumpling will be of pure bending [33]. Hence, for self-avoiding membranes ($\gamma\to\infty, \kappa\to 0$), the scaling exponent β is expected to be $\beta_{\rm sa}=0.025\ll\delta_{\rm sa}=0.25$, whereas for self-avoiding sheets of finite rigidity (thickness) it was found that $\beta_{\rm sa}^R=0.06\pm0.005\approx\beta_{\rm ph}=1/16=0.0625$, i.e., it is almost the same as for phantom membranes; nevertheless, $\delta_{\rm sa}^R\approx\delta_{\rm sa}=0.25<\delta_{\rm ph}=0.375$ [8]. So the stretching of the folded sheet diminishes the effect of self-avoidance. Accordingly, the values of $\mu=\nu>\nu_{\rm sa}=0.8$ can be attributed to the decrease in the effect of short-range self-avoiding interactions for thin sheets with finite rigidity (see Table I), whereas the values of $\mu=\nu<\nu_{\rm ph}=0.75$ can be attributed to the competition between bending and stretching in the more thick and rigid sheets (see Table I).

The scaling behavior (15) also explains the intrinsically anomalous nature of crumpled sheet roughness. Namely, we found that each individual crumpled sheet possesses a self-affine invariance within a bounded interval of length scales with the sheet size dependent lower cutoff $\Delta_C\cong\Delta_R$, such that at scales $\Delta<\Delta_C$ the crumpled sheet is essentially flat ($\zeta=1$), whereas at larger scales the sheet roughness is characterized by the local roughness exponent $\zeta=0.72\pm0.04$, which is found to be the same for all papers used in this work. In contrast to this, the scaling behavior (15) of the cutoff $\Delta_C\cong\Delta_R$ leads to the power-law dependence of sheet roughness on the sheet size (13) with the material dependent global roughness exponent $\alpha=\mu$ [see Eqs. (14) and (16)]. Consequently, the ensemble of crumpled sheets of different sizes displays an intrinsically anomalous roughness with the global roughness exponent $\alpha=\mu>\zeta$. Another important finding of this work is that the sheet roughness in the folded and unfolded states is characterized by the same roughness expo-

nents. Notice that the finding $\alpha \geq \zeta > 0.5$ indicates that the configurations of crumpled sheets are not random; rather they are characterized by the long-range correlations in the local and global scales [31].

It should be pointed out that the universality of the local roughness exponent is consistent with the concept of universality classes in kinetic roughening [34]. We note that our finding $\zeta = 0.72 \pm 0.04$ is consistent with the universal roughness exponent $\zeta = 0.71 \pm 0.01$ reported in [2], whereas the value of roughness exponent 0.88 ± 0.06 reported in [11] can be associated with the material dependent global roughness of crumpled paper (see Table I). Besides, we note the numerical coincidence of $\zeta = 0.72 \pm 0.04$ with $\nu_{\mathrm{ph}} = 0.75$ indicating that self-avoiding interactions do not affect sheet roughening in the local scale, whereas the case of global roughness is determined by the short-range self-avoiding interactions [35], if $\mu \geq \nu_{\mathrm{sa}} = 0.8$. On the other hand, if the sheet crumpling geometry is governed by the long-range elastic interactions, the crease length scaling exponent is $\mu < \nu_{\mathrm{ph}} = 0.75$ and so the sheet roughness is expected to display a self-affine invariance within a bounded range of length scale, i.e., $\alpha = \zeta = \nu_{\mathrm{ph}}$, as it is observed for crumpled Albanene-2 paper (see Table I).

IV. CONCLUSIONS

Our findings suggest that the fractal geometry of randomly crumpled thin sheets is determined by the scaling properties of the crumpling network accumulating the energy of external crumpling forces. Specifically, we found that the mass fractal dimension of randomly folded balls is determined by the power law dependence of the mean crease length on the sheet size (15), such that $D_M = 2/\mu$. Besides, the surfaces of crumpled balls and unfolded crumpled sheets both exhibit self-affine invariance, if $\mu \leq \nu_{\mathrm{ph}}$, or an intrinsically anomalous roughness, if $\mu < \nu_{\mathrm{ph}}$. In both cases the local roughness is characterized by the universal local roughness exponent $\zeta \approx \mu_{\mathrm{ph}} = 0.75$, whereas the global roughness exponent (in the case of anomalous roughness) is found to be material dependent. Specifically, we found that $\alpha = \mu = \nu = 2\beta + 1 - \delta$ for $\mu < \nu_{\mathrm{ph}}$. This means that the crumpling configurations of elastoplastic sheets are determined by the competition between bending and stretching deformations in the folded sheet; nevertheless, the local geometry of crumpling is universal. These findings offer an insight into the nature of crumpling phenomena.

ACKNOWLEDGMENT

This work has been supported by CONACyT of the Mexican Government under Project No. 44722.

[1] B. A. DiDonna and T. A. Witten, Phys. Rev. Lett. **87**, 206105 (2001); K. Matan, R. B. Williams, T. A. Witten, and S. R. Nagel, *ibid.* **88**, 076101 (2002); E. Cerda and L. Mahadevan, *ibid.* **90**, 074302 (2003); A. Aström, J. Timonen, and M. Karttunen, *ibid.* **93**, 244301 (2004); A. S. Balankin *et al.*, Phys. Rev. E **73**, 065105(R) (2006).

[2] D. L. Blair and A. Kudrolli, Phys. Rev. Lett. **94**, 166107 (2005).

[3] E. Sultan and A. Boudaoud, Phys. Rev. Lett. **96**, 136103 (2006).

[4] A. E. Lobkovsky, S. Gentges, H. Li, D. Morse, and T. A. Witten, Science **270**, 1482 (1995); E. M. Kramer and T. A. Witten, Phys. Rev. Lett. **78**, 1303 (1997); G. Gompper, Nature (London) **386**, 439 (1997); M. B. Amar and Y. Romeau, Proc. R. Soc. London, Ser. A **453**, 729 (1997).

[5] *Witten's Lectures on Crumpling*, edited by A. J. Wood, Special issue of Physica A **313**, 83 (2002).

[6] K. Matan, R. B. Williams, T. A. Witten, and S. R. Nagel, Phys. Rev. Lett. **88**, 076101 (2002).

[7] R. F. Albuquerque and M. A. F. Gomes, Physica A **310**, 377 (2002); R. Cassia-Mouraa and M. A. F. Gomes, J. Theor. Biol. **238**, 331 (2006).

[8] G. A. Vliegenthart and G. Gompper, Nat. Mater. **5**, 216 (2006).

[9] M. A. F. Gomes, Am. J. Phys. **55**, 649 (1987); J. Phys. A **20**, L283 (1987); **23**, L1281 (1990); M. A. F. Gomes, G. L. Vasconcelos, and C. C. Nascimento, *ibid.* **20**, L1167 (1987).

[10] M. A. F. Gomes and J. H. P. Soares, J. Phys. D **22**, 989 (1989); M. A. F. Gomes *et al.*, *ibid.* **22**, 1217 (1989).

[11] F. Plouraboué and S. Roux, Physica A **277**, 173 (1996).

[12] I. Peterson, Sci. News (Washington, D. C.) (Washington, D.C.) **163**, 524 (2003).

[13] T. A. Vilgis, J. Phys. II **2**, 92 (1992); F. David and K. J. Wiese, Phys. Rev. Lett. **76**, 4564 (1996).

[14] R. H. Ko and C. P. Bean, Phys. Teach. **29**, 78 (1991).

[15] Y. Kantor, M. Kadar, and D. R. Nelson, Phys. Rev. Lett. **60**, 238 (1988).

[16] V. S. Ivanova, A. S. Balankin, I. J. Bunin, and A. A. Oksogoev, *Synergetics and Fractals in Material Science* (Nauka, Moscow, 1994).

[17] As far as we know, no experimental data for the roughness exponent of crumpled ball surfaces have been reported.

[18] P. A. Houle and J. P. Sethna, Phys. Rev. E **54**, 278 (1996).

[19] A. S. Balankin *et al.*, Proc. R. Soc. London, Ser. A **455**, 2565 (1999); A. S. Balankin, O. Susarrey, and A. Bravo, Phys. Rev. E **64**, 066131 (2001); A. S. Balankin, O. Susarrey, and J. M. Gonzáles, Phys. Rev. Lett. **90**, 096101 (2003); A. S. Balankin *et al.*, *ibid.* **96**, 056101 (2006).

[20] M. Alava and K. Niskanen, Rep. Prog. Phys. **69**, 669 (2006).

[21] The goodness-of-fit tests with the chi-squared, Kolmogorov-Smirnov, and Anderson statistics were performed with the help of @RISK software (http://www.palisade.com).

[22] After relaxation, the variations in the ensemble averaged diameter of balls folded by different persons are found to be less than the statistical variations of the mean diameter (±5%); nevertheless, the variations in the initial confinement ratio achieve 25%.

[23] It should be pointed out that papers used in this work are

characterized by the low capacity of water absorption.
[24] A. Brú *et al.*, Phys. Rev. Lett. **81**, 4008 (1998); **92**, 238101 (2004).
[25] A. S. Balankin and O. Susarrey, Philos. Mag. Lett. **79**, 629 (1999); A. S. Balankin *et al.*, Phys. Rev. E **72**, 065101(R) (2005).
[26] http://www.sciocorp.com (SCION-IMAGE, 1999).
[27] We note that the gamma distribution also provides a quite good adjustment [see Fig. 4(c)] and cannot be clearly rejected in terms of χ^2, Kolmogorov-Smirnov, and Anderson statistics.
[28] J. J. Ramasco, J. M. López, and M. A. Rodríguez, Phys. Rev. Lett. **84**, 2199 (2000).
[29] A. S. Balankin, D. M. Matamoros, and I. Campos, Philos. Mag. Lett. **80**, 165 (2000).
[30] F. Falconer, *Fractals* (Plenum Press, New York, 1988).
[31] We noted that μ depends on the bending rigidity of paper as $\mu \propto \kappa^{-1}$.
[32] A. S. Balankin, Sov. Tech. Phys. Lett. **17**, 532 (1991); Phys. Rev. B **53**, 5438 (1996).
[33] E. Cerda and L. Mahadevan, Proc. R. Soc. London, Ser. A **461**, 671 (2005).
[34] A.-L. Barabási and N. E. Stanley, *Fractal Concepts in Surface Growth* (Cambridge University Press, Cambridge, UK, 1995).
[35] M. J. Bowick and A. Travesset, Phys. Rep. **344**, 255 (2001) and references therein.